

Recrystallization in AISI 304 austenitic stainless steel during and after hot deformation

A. Dehghan-Manshadi^{a,b,*}, M.R. Barnett^b, P.D. Hodgson^b

^a Faculty of Engineering, University of Wollongong, NSW, Australia

^b Centre for Materials and Fibre Innovation, Deakin University, Waurn Ponds, VIC, Australia

Received 21 February 2007; received in revised form 14 August 2007; accepted 15 August 2007

Abstract

In order to improve the understanding of the dynamic and post-dynamic recrystallization behaviours of AISI 304 austenitic stainless steel, a series of hot torsion test have been performed under a range of deformation conditions. The mechanical and microstructural features of dynamic recrystallization (DRX) were characterized to compare and contrast them with those of the post-dynamic recrystallization. A necklace type of dynamically recrystallized microstructure was observed during hot deformation at 900 °C and at a strain rate of 0.01 s⁻¹. Following deformation, the dependency of time for 50% recrystallization, t_{50} , changed from “strain dependent” to “strain independent” at a transition strain (ε^*), which is significantly beyond the peak. This transition strain was clearly linked to the strain for 50% dynamic recrystallization during deformation. The interrelations between the fraction of dynamically recrystallized microstructure, the evolution of post-dynamically recrystallized microstructure and the final grain size have been established. The results also showed an important role of grain growth on softening of deformed austenite.

© 2007 Elsevier B.V. All rights reserved.

Keywords: Stainless steel; Hot deformation; Dynamic recrystallization; Post-dynamic recrystallization; EBSD

1. Introduction

The evaluation of microstructure development during and after hot deformation of metallic materials has practical importance due to its relationship with mechanical properties of final products. Several different processes, such as dynamic recovery (DRV), dynamic recrystallization (DRX), static recrystallization (SRX) and post-dynamic recrystallization, can influence the microstructure of deformed material.

Dynamic recrystallization, which is the process of formation of new small and dislocation free grains from deformed material, usually takes place in materials with low to medium stacking fault energy (SFE) such as austenitic stainless steel [1]. The general descriptive model for DRX is that during deformation, the pre-existing grain boundaries elongate along the deformation direction, grain boundary serrations appear and then new DRX grains nucleate at the serrated parts of grain boundaries (i.e. bulging). The nucleation of these DRX grain can start at a critical strain, ε_c , which is a function of initial microstructure and deformation conditions. Then, the evolution of DRX microstructure can proceed further by increasing deformation and through the formation of a necklace structure [1,2]. It has been shown that deformation conditions, temperature and strain rate, have pronounced effects on the DRX necklace structure and DRX (or steady state) grain size [3–5], but the effect of the initial grain size is wiped out [6,7]. Although the progress of DRX based on a necklace structure has been observed in several different materials [1,2,8], the exact mechanism (especially for the formation of second layers) and also the hot deformation conditions which cause formation of such structure are not well understood.

The partial DRX microstructure is usually contains a high dislocation density. The presence of these dislocations provides the driving force for interpass and/or post-deformation softening. Recrystallization of a structure containing some degree of DRX may include classical static recrystallization, which involves nucleation and growth of new strain free grains, and/or post-dynamic recrystallization. The sensitivities of the kinetics of these two types of recrystallization (i.e. SRX and post-DRX) to processing parameters can be quite different [9–11]. At high strains, where it has been suggested that post-DRX is dominant, the kinetics of softening is independent of strain, strongly

The partial DRX microstructure is usually contains a high dislocation density. The presence of these dislocations provides the driving force for interpass and/or post-deformation softening. Recrystallization of a structure containing some degree of DRX may include classical static recrystallization, which involves nucleation and growth of new strain free grains, and/or post-dynamic recrystallization. The sensitivities of the kinetics of these two types of recrystallization (i.e. SRX and post-DRX) to processing parameters can be quite different [9–11]. At high strains, where it has been suggested that post-DRX is dominant, the kinetics of softening is independent of strain, strongly

* Corresponding author.

E-mail addresses: alidm@uow.edu.au (A. Dehghan-Manshadi), matthew.barnett@deakin.edu.au (M.R. Barnett), peter.hodgson@deakin.edu.au (P.D. Hodgson).

dependent on strain rate and depend weakly on temperature and composition [12–15]. At low strains, where SRX is proposed as the most important softening mechanism, the kinetics are strong functions of temperature, strain and grain size and only weakly depend on strain rate [9,16]. There is usually a transition strain, ε^* , where the softening behaviour of deformed material changes from *strain dependent* (low strain) to *strain independent* (high strain). This transition strain normally falls between the critical strain for initiation of DRX, ε_c , and the strain for the steady state, ε_{ss} , and is often close to the strain for the peak stress, ε_p [17–19]. It has been proposed [14] that all of the recrystallization nuclei are present at the end of deformation for any strains higher than ε^* and, because of the steady state nature of DRX, further working does not lead to any more nuclei. This leads to an expectation of a weak strain dependency of recrystallization in the strain independent region. However, the exact requirement for transition from strain dependent to strain independent is still a matter of debate.

Many works were previously done to understand DRX and post-DRX in several metallic and non-metallic alloys (e.g. [20–22]). Austenitic stainless steels with a low value of SFE (~ 21 J/mol at room temperature [1]) have always been an important model alloy for DRX and post-DRX investigations over the last decades [23–27]. However, there are still some unclear issues on recrystallization of this material. The evolution of DRX and especially post-DRX grain size, the correlation between DRX fraction and post-DRX kinetics and the role of grain growth on post-deformation softening are some example of those unclear issues. The aim of this study is to investigate the dynamic and post-dynamic recrystallization processes of austenite in AISI 304 stainless steel and interrelationship between these two phenomena, in order to improve understanding on those unclear aspects of recrystallization.

2. Experimental methods

AISI 304 austenitic stainless steel with a chemical composition (wt%) of Fe–0.02% C–1.6% Mn–8.2% Ni–18.5% Cr–0.8% Cu was used in this study. Torsion samples with a gage length of 20 mm and a diameter of 6.7 mm were machined from the rolled bars. The torsion equipment used in this study has been described elsewhere [28]. Hot torsion tests were carried out according to the schedule illustrated in Fig. 1. The samples were heated to 1200 °C at 5 °C s^{−1} and held for 3 min. A roughing process using a strain of 0.5, at a strain rate of 1 s^{−1} followed by 120 s holding time was applied and this resulted in a homogenized microstructure with an average grain size of ~ 35 μ m. The samples were then cooled at 1 °C s^{−1} to various temperatures in the range of 850–1100 °C, held for 2 min and deformed at strain rates between 0.001 and 1 s^{−1} to different strains. The samples were quenched immediately (<0.5 s) after deformation (Fig. 1a) to investigate the DRX microstructure, whereas, to investigate the post-deformation recrystallization microstructure, the samples were quenched after un-loading for different times at the deformation temperature (Fig. 1b). Metallographic observations were performed on tangential sections at a depth of ~ 100 μ m below the sample surface. Electron backscattered diffraction (EBSD)

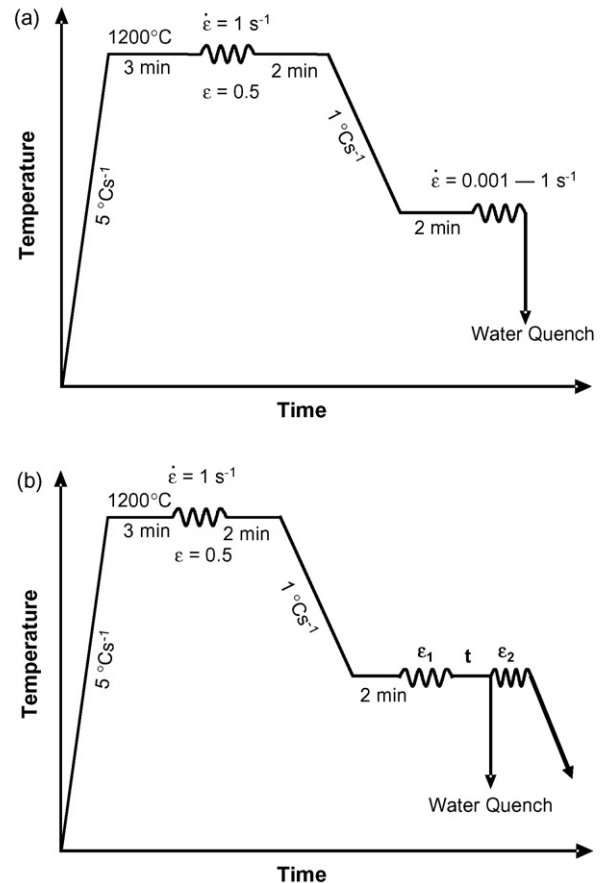


Fig. 1. Schematic diagrams of hot deformation tests for (a) DRX studies and (b) post-DRX studies.

under an accelerating voltage of 20 kV, a working distance of 25 mm from the gun and an aperture size of 60 μ m was used to analyse the microstructure. The EBSD maps were generated by the controlled movement of the beam over a grid pattern with a step size of 0.5 μ m at a magnification of 1000 \times and then analysed using HKL technology channel 5 software.

The softening was measured by reloading the specimen to a strain of 0.2 after different un-loading times (Fig. 1b). The softening fraction ($X\%$) was determined using the 0.2% offset strain method:

$$X(\%) = \frac{\sigma_m - \sigma_2}{\sigma_m - \sigma_1} \times 100 \quad (1)$$

where σ_m is the stress at the end of first deformation, and σ_1 and σ_2 are the 0.2% offset stress for the first and second deformations, respectively. It has been shown [29] that this method can predict the softening fraction more accurately than other methods, such as back extrapolation or mean flow stress, because of the avoidance of short recovery transient.

3. Results

3.1. Deformation behaviour

A number of stress–strain (σ – ε) curves obtained for different temperatures and strain rates are shown in Fig. 2. All of the

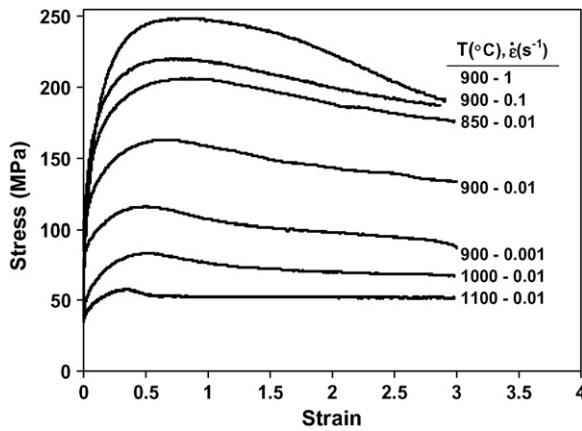


Fig. 2. Stress–strain curves at different deformation temperatures and strain rates.

samples exhibited typical DRX flow curves with a single peak stress followed by a gradual fall towards a steady state stress. However, at deformation temperatures below 900 °C or strain rates higher than 0.01 s^{−1}, there appears to be softening beyond the peak due to deformation heating or, in some cases, localization of strain and/or sample failure. However, at very low strain rate of 0.01 s^{−1} the effect of deformation heating is negligible [29]. It can be seen that the peak becomes less obvious when the deformation temperature is decreased or strain rate increased.

The flow curves were analysed using the work hardening rates, $\theta = \partial\sigma/\partial\epsilon$, as a function of stress (Fig. 3). These work hardening curves consist of two stages. In the first stage, the work hardening rate decreases rapidly with increasing stress due to dynamic recovery, up to the initiation of a second stage, where DRX is considered to start and where a noticeable change occurs in the slope of the curve. This slope change is used to identify a critical stress, σ_c , and strain, ϵ_c , for initiation of DRX. The details of this method have been explained elsewhere [27,30,31].

The activation energy of deformation, Q , can be estimated by fitting a hyperbolic sine function to the stress corresponding to the peak, as first proposed by Sellars and McTegart [32]:

$$Z = A[\sinh(\alpha\sigma)]^n = \dot{\epsilon} \exp\left(\frac{Q}{RT}\right) \quad (2)$$

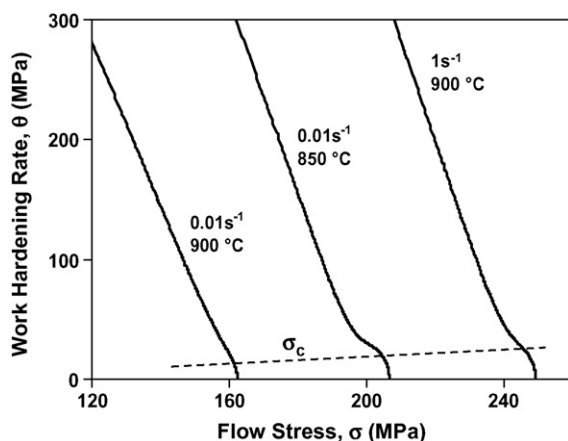


Fig. 3. Work hardening rate as a function of flow stress ($Q_{\text{def}} = 400$ kJ/mol).

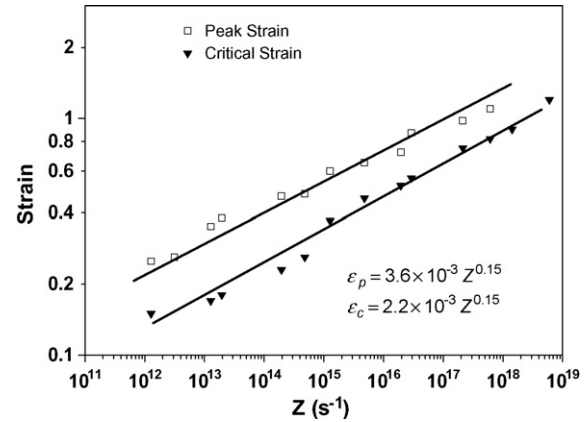


Fig. 4. Peak and critical strains as functions of Zener–Hollomon parameter.

where $\dot{\epsilon}$ is the strain rate (s^{−1}), A , α and n are constants independent of temperature, σ is the stress (MPa), Q is the hot deformation activation energy (J/mol), R is the gas constant and T is the absolute temperature (K) of deformation. A value of 400 kJ/mol was obtained for this steel, which is in good agreement for 304 austenitic stainless steels reported by others [27,33,34]. This activation energy (through the Zener–Hollomon parameter) can, usually, be used to predict constitutive equations for strain to the peak stress, commonly termed the peak strain (ϵ_p) and critical strain (ϵ_c) for initiation of DRX (Fig. 4). It can be seen that $\epsilon_c \sim 0.6\epsilon_p$ for most of the deformation conditions studied here.

The DRX microstructure after quenching at different deformation conditions was analysed by EBSD. The initial microstructure, obtained after roughing, consisted of equiaxed grains with a large quantity of twin boundaries (Fig. 5). These equiaxed grains are the result of static recrystallization and grain growth following roughing. The presence of such a high quantity of twin boundaries in the microstructure demonstrates the formation of twins during recrystallization of this steel, as is well established [2,35–37].

Deformation of this initial microstructure to a low strain (Fig. 6a), caused elongation of the equiaxed grains in the deformation direction. The grain boundaries started to serrate, and this serration, as well as elongation of grains, increased with increas-

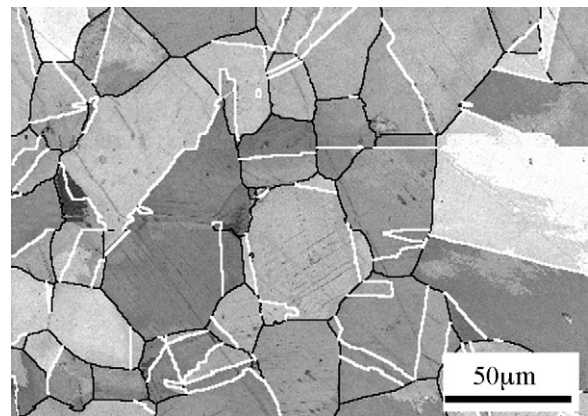


Fig. 5. EBSD maps of a sample after roughing process and cooling to 900 °C (the initial microstructure before hot deformation). High angle ($\theta > 15^\circ$) and twin boundaries shown by black and white lines, respectively.

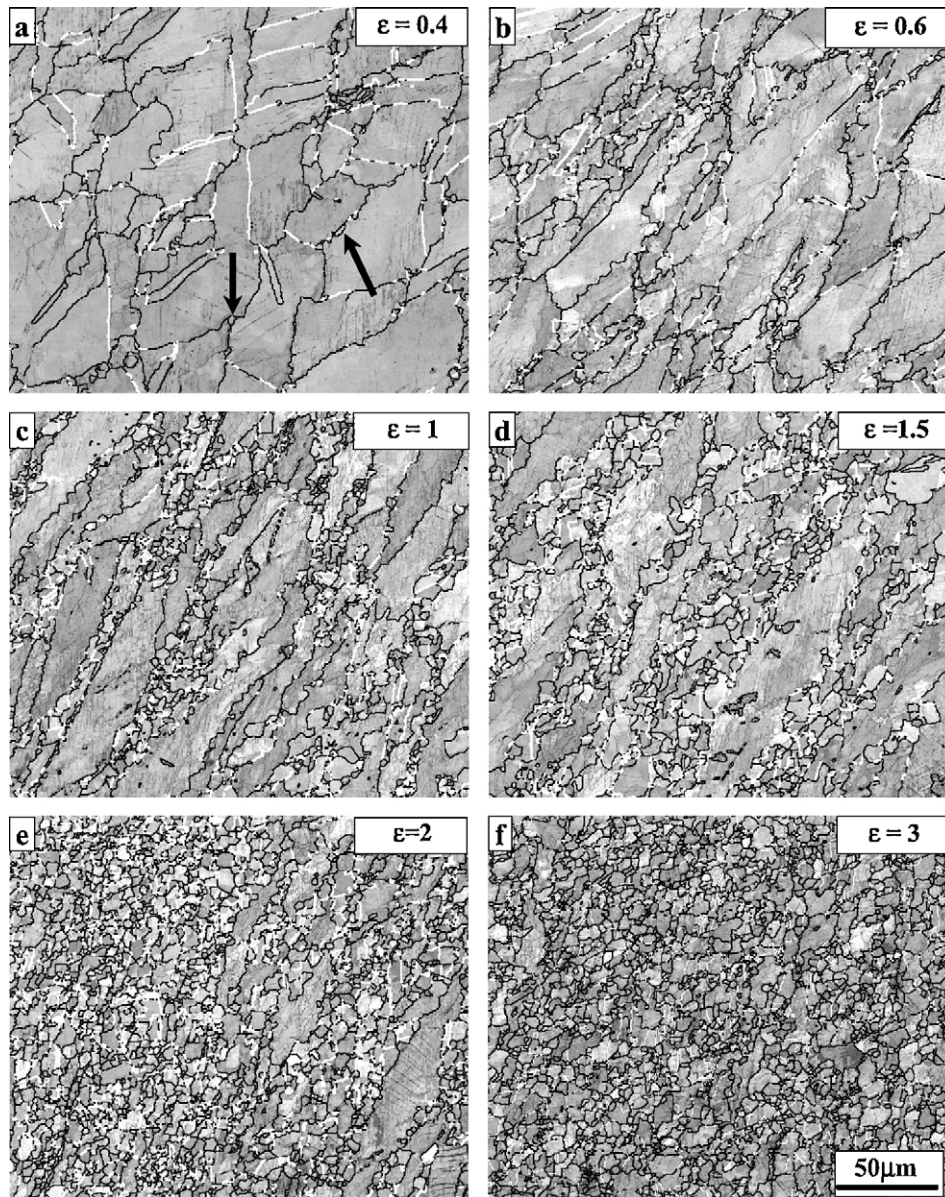


Fig. 6. EBSD maps of samples deformed at 900 °C and strain rate of 0.01 s⁻¹. High angle ($\theta > 15^\circ$) and twin boundaries shown by black and white lines, respectively ($\varepsilon_c = 0.45$; $\varepsilon_p = 0.8$).

ing strain. However, the first evidence of DRX is also obvious by the formation of a limited number of new small grains at this strain (arrows in Fig. 6a). More new small grains were formed with deformation to higher strain (Fig. 6b). With increasing strain beyond the peak, most of the pre-existing boundaries were decorated by these new DRX grains and the first layer of a necklace structure had formed (Fig. 6c). There is extensive evidence for the formation of the first layer of this necklace structure (along the pre-existing grain boundaries) through the bulging mechanism [23,33,38,39]. With increasing strain, more DRX grains form on the interface of the first necklace layer and un-recrystallized material (i.e. at the recrystallization front) and the second layers of the necklace structure start to form (Fig. 6d). However, it is also clear that in some grains the original austenite boundary shows no evidence of DRX; this highlights that there is an inhomogeneity in the DRX process.

Whether the formation of these second layers of the necklace structure is by the same mechanism as first layer (bulging) is still a matter of debate [39]. The formation of new grains continued with further deformation and without any major change in the DRX grain size (Fig. 6e). Finally, at the steady state strain, a nearly complete DRX microstructure has formed (Fig. 6f), although, some non-recrystallized areas remained in the microstructure, even at the fracture strain.

It is generally believed [40] that growth of the DRX grains is limited by work hardening in the grain interior, which is greater at lower temperatures and higher strain rates (i.e. at high Z values). Therefore, the microstructures of samples deformed under high Z conditions are finer than those of the samples deformed under low Z values. The DRX grain size (D_{DRX}) is often given as a power law function of the Zener–Hollomon parameter. The present grain sizes follow this relationship and are given along

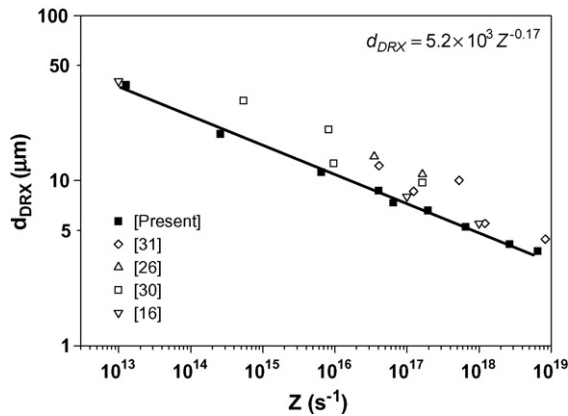


Fig. 7. DRX grain size as a function of Zener–Hollomon parameter.

with some literature values in Fig. 7. Once corrected to mean grain diameter values (i.e. the mean linear intercept multiplied by 1.68 [41]), there is a relatively good agreement between the present data and previous work [26,27] for different ranges of grain sizes and deformation modes. The remaining differences can be ascribed to the different metallography methods. The literature values were obtained using optical metallography, whereas the present data were obtained using EBSD. The difficulty in etching the boundaries in stainless steels means that optical metallography tends to over estimate the grain size.

3.2. Post-deformation behaviour

Double-twist tests were performed to investigate the post-dynamic recrystallization process at a deformation temperature of 900 °C and a strain rate of 0.01 s^{−1} for different strains and un-loading times. In the case of short un-loading times, the softening was negligible and the flow curves of the second twist followed the expected path of the initial flow curve (Fig. 8). For longer un-loading times, near complete softening occurred and, in some cases, a peak was seen in the second twist flow curves, where these peak strains were smaller than the peak strains in the first twist flow curves. This reduction in ϵ_p (and σ_p) can be ascribed to the grain refinement that occurs during recrystallization [7,42]. In fact, in the microstructure with smaller grain size (as the initial microstructure for the second deformation) DRX can start faster (lower strain) and also proceeds with a higher kinetics. However, the effect of stored energy in the partially recrystallized material is considerable.

The fractional softening was measured as a function of un-loading time for different applied strains and for a given deformation condition (Fig. 9). The volume fraction of DRX for the same deformation condition is also superimposed on this plot by converting strain to the time. The softening follows a typical sigmoidal behaviour and, within the scatter of the present data, this holds for all strains. The times for 50% softening (t_{50}) showed that softening decreased with strain up to a transition strain (ϵ^*) where the softening becomes strain independent (Fig. 10). The effect of temperature in the strain dependent regions ($\epsilon < \epsilon^*$) is stronger than its effect on the strain independent region ($\epsilon > \epsilon^*$). This difference is in agreement with the observations reported by many authors [3,9,14].

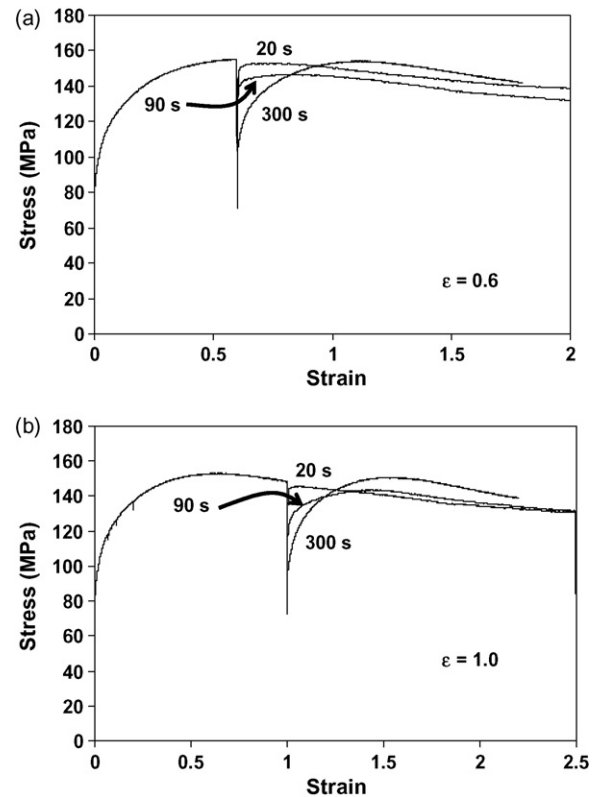


Fig. 8. Double-twist flow curves obtained at deformation temperature of 900 °C, strain rate of 0.01 s^{−1}, different strain and un-loading times.

At a given strain, the time for 50% recrystallization increased with decreasing strain rate (Fig. 11). However, in this case, the effect of strain rate is greater at high strains (strain independent region), which again agrees with most observations [14,43]. For the sake of comparison, the volume fraction of DRX for strain rates of 0.01 and 1 s^{−1} is superimposed on the plot. In each case ϵ^* corresponds to about 50% volume fraction of DRX.

To further investigate the post-deformation recrystallization, EBSD analysis was performed on samples tested at 900 °C and

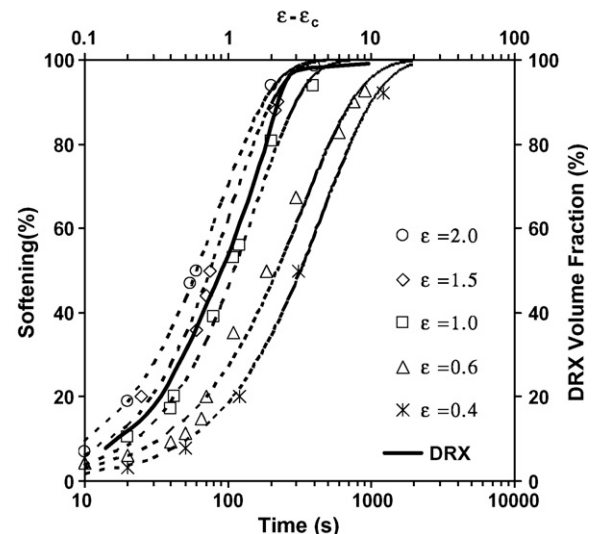


Fig. 9. The effect of applied strain on the softening fraction at deformation temperature of 900 °C and a strain rate of 0.01 s^{−1}.

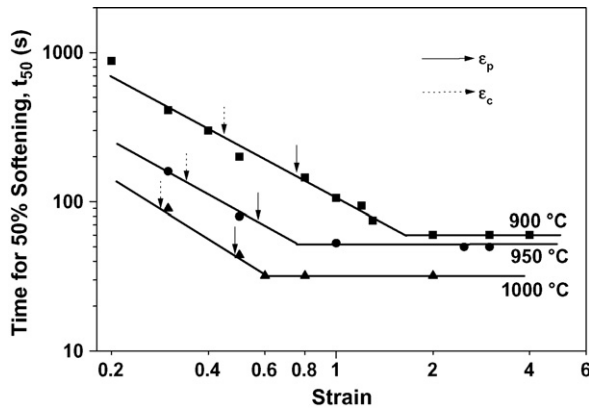


Fig. 10. The time for 50% softening after deformation at different temperatures and a constant strain rate of 0.01 s^{-1} .

a strain rate of 0.01 s^{-1} and quenched after different un-loading times (Fig. 12). At a strain lower than ε_c (i.e. $\varepsilon = 0.4$), where the deformed microstructure (Fig. 6a) consisted of slightly elongated grains with a small degree of grain boundary serration, a limited number of new small grains formed on the serrated pre-existing grain boundaries after holding for a short time (Fig. 12a). The formation of these new grains is assumed to be an indication of SRX. These grains grew and eventually filled the deformed structure at higher degrees of softening (Fig. 12b and c).

At a strain just beyond the peak ($\varepsilon = 1.0$), where DRX occurred during deformation and many small DRX grains ($\sim 20\%$ of volume) were observed at pre-existing grain boundaries immediately following hot deformation (Fig. 6c), the microstructure after a short interpass time consisted of a high fraction of recrystallized grains (Fig. 12d). These new grains were noticeably coarser than the DRX grains (compare with Fig. 6b). With increasing time, the average grain size near the original grain boundaries increased (Fig. 12e) and finally, the microstructure was replaced by a relatively equiaxed microstructure with an average grain size of $\sim 15 \mu\text{m}$ (Fig. 12f).

After a high strain ($\varepsilon = 2.0$) into the steady state region, where most of the initial microstructure comprised DRX grains

(Fig. 6e), softening was accompanied by an increase in the average grain size (Fig. 12g and h) with no discernible nucleation and growth of new grains. The frequency of high angle boundaries with a twin crystallography also considerably increased with increasing time.

4. Discussion

The evolution of DRX microstructure based on the necklace structure has been known as the most likely DRX mechanism during hot deformation of austenite [1,2]. Several different parameters, such as deformation conditions and initial microstructure, can cause a departure from a necklace structure, but the microstructure obtained at 900°C and a strain rate of 0.01 s^{-1} showed a well-developed necklace structure. This DRX structure, on the other hand, and specifically its volume fraction, has an important role in the development of post-DRX microstructure. The current work on both DRX and post-DRX structures, revealed some key observations that differ with those obtained previous studies. Firstly, the change from strain dependent to strain independent recrystallization occurred at a strain significantly beyond the peak. In most works [18,19] it is assumed that ε^* is very close to ε_p , although other recent work [44] for a HSLA steel showed the ratio of ε^* to ε_p can vary widely as the ratio of dynamic to initial grain size changed. Here, the change in the post-deformation recrystallization behaviour from strain dependent to strain independent appears to be closely linked to the strain for 50% dynamic recrystallization during deformation. Fig. 11 shows that at a strain equal to ε^* almost 50% DRX occurred in the deformed materials under both strain rates of 0.01 and 1.0 s^{-1} . It is likely that this may vary depending upon the initial grain size. Finally, it is noted that there are clear differences in the recrystallized grain size as a function of DRX fraction (or strain) depending upon the state of the microstructure at the end of deformation.

Each of these aspects, as well as the general recrystallization behaviours are discussed below.

4.1. Dynamic recrystallization

The initiation and progress of the DRX microstructure based on the necklace structure is obvious during deformation at 900°C and 0.01 s^{-1} (Fig. 6). Under this condition the dynamically recrystallized grain size ($7.5 \mu\text{m}$) is much smaller than the initial grain size ($35 \mu\text{m}$). The rate of DRX in this alloy and its effect on the flow curve is somewhat different to other steels. At the peak strain ($\varepsilon_p = 0.8$) only 15% DRX had occurred and even at a strain significantly beyond the peak (e.g. $\varepsilon = 1.5$) there was less than 50% recrystallization, with some initial boundaries still apparent (Fig. 6d). In this case, a nearly full DRX microstructure is only obtained after deformation to a strain higher than 2 (Fig. 6e). The kinetics of the DRX process depends on the deformation conditions of temperature and strain rate, as well as the initial microstructure (grain size) and can be modelled using a modified Avrami type equation:

$$X = 1 - \exp(-k(\varepsilon - \varepsilon_c)^n) \quad (3)$$

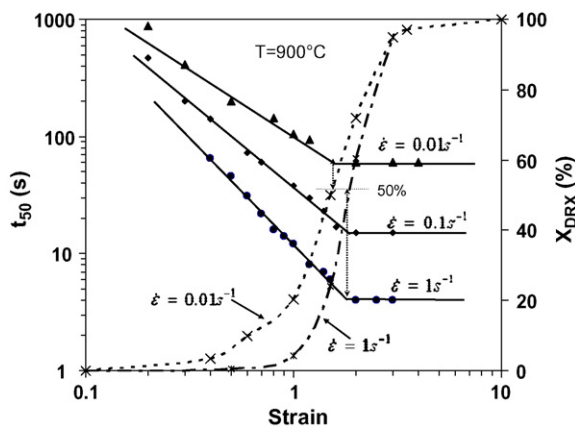


Fig. 11. The time for 50% softening after deformation at different strain rates as a function of applied strain. Also superimposed are the DRX volume fraction for strain rates of 0.01 and 1.0 s^{-1} .

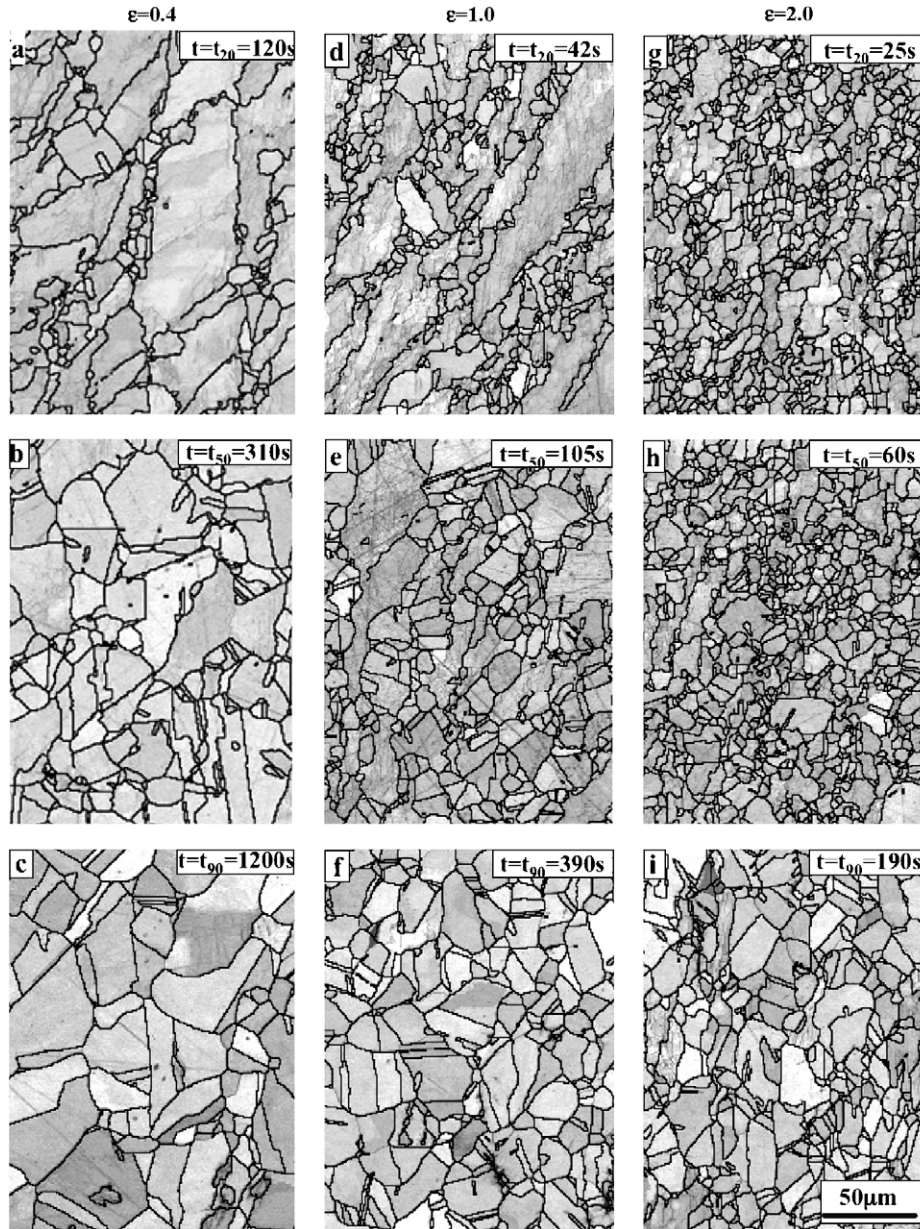


Fig. 12. EBSD maps of samples deformed at 900 °C and held for different times after deformation ($\dot{\epsilon} = 0.01 \text{ s}^{-1}$) to produce softening levels of 20, 50 and 90%.

where n is a constant and k typically depends on temperature, strain rate and initial grain size. At a constant initial grain size the value of k was found to correlate with strain rate and temperature as follows [45]:

$$k = k_0 \dot{\epsilon}^\alpha \exp\left(\frac{Q}{RT}\right) \quad (4)$$

where k_0 and α are constants and Q is the activation energy. The present data can be fitted using a value of $n \sim 1.3$. This value is in good agreement with values proposed by other researchers using mechanical [27] and/or optical metallography [41] measurements. However, this n value is significantly lower than the range of 1.5–2.5 generally reported for plain carbon or low alloy steels [45,46]. This implies a lower DRX rate in stainless steel.

4.2. Post-dynamic recrystallization

Similar to deformation period, the kinetics of softening during the post-deformation period are functions of strain rate and temperature. These kinetics are usually presented as a function of time for 50% softening (t_{50}) in the form of an Avrami equation [3]:

$$X = 1 - \exp\left[-0.693\left(\frac{t}{t_{50}}\right)^m\right] \quad (5)$$

with

$$t_{50} = A \dot{\epsilon}^{-p} Z^{-q} \exp\left(\frac{Q_{\text{rex}}}{RT}\right) \quad (6)$$

where X is the recrystallization fraction, t is un-loading time (s), m is the Avrami constant for post-DRX, t_{50} is the time for 50% softening (s), Z is Zener–Hollomon parameter and Q_{rex} is the activation energy for recrystallization (J/mol). The Avrami exponent value, m , was about 1.1 which is close to the Avrami exponent of dynamic recrystallization in Eq. (3). Interestingly, in contrast to the DRX process, this m value is in the range of 0.8–1.3 usually reported for post-DRX in other steels [14,47].

From estimation of the activation energy and the exponents of Eq. (6) the following equations can be developed for the strain dependent and independent regions, respectively:

$$t_{50} = 8 \times 10^{-9} \varepsilon^{-1.5} Z^{-0.42} \exp \left(\frac{375,000}{RT} \right) \quad (7)$$

$$t_{50} = 2.7 \times 10^{-2} Z^{-0.61} \exp \left(\frac{292,000}{RT} \right) \quad (8)$$

In the above approach it was assumed that the strain rate sensitivity must act through Z rather than as an independent function of strain rate. This means that some account of this must be taken when comparing with other workers; particularly as it affects Q_{rex} . The reason for this is that from the raw data there will be an apparent activation energy that is obtained from plots of t_{50} versus $1/T$ for a given strain. In this case, for example for the strain independent region $Q_{\text{app}} = Q_{\text{rex}} - 0.16Q_{\text{def}}$, and therefore, from Eq. (8), Q_{app} is ~ 50 kJ/mol for the strain independent region. This reflects the general observation of a lack of, or very low, temperature dependence in this region. The difference in recrystallization activation energies in Eqs. (7) and (8) is significant and indicate different mechanisms of recrystallization, and also may arise from some error in assuming that strain rate sensitivity must be incorporated through Z .

A comparison between the DRX kinetics and post-DRX softening is presented in Fig. 9 for a given temperature and strain rate. The position of the DRX curve, which is close to the softening curve related to the pre-strain of 1.5, implies that when the nucleation period is eliminated from the DRX process (by subtracting ε_c from ε), the DRX kinetics are very similar to post-DRX. This suggests that with deformation to a strain of 1.5 the dislocation density in the deformed structure reached a saturation value and softening of such a structure (during un-loading) can occur just by the post-DRX mechanism (i.e. growth of DRX nuclei). Overall, this also implies that the natures of the DRX and post-DRX processes are very similar. The position of the DRX curve in such plots, as well as ε^* , is a function of strain rate and temperature. A comparison between Figs. 10 and 11 shows the strong dependency of this strain (ε^*) to temperature and a lower sensitivity to strain rate. This effect can be attributed to increased mobility of grain boundaries (growth kinetics) with increasing temperature. On the other hand, as previously showed in Fig. 11 the current study indicated a tight relationship between the transition strain and the volume fraction of recrystallized microstructure during deformation (i.e. DRX fraction). Fig. 13 interestingly shows that for all deformation condition tested here, a microstructure with $\sim 50\%$ dynamic recrystallized grains corresponded with the transition from strain dependent to strain independent behaviour. This 50% volume

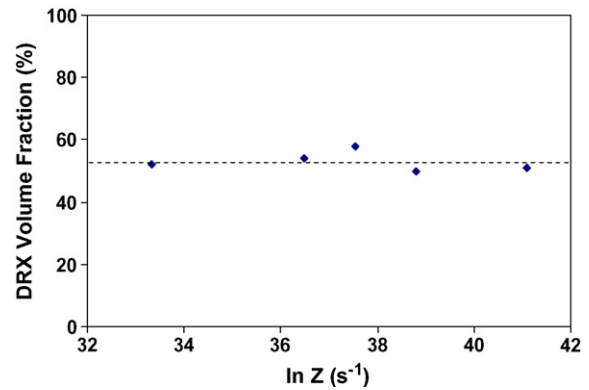


Fig. 13. DRX fraction at a strain equal to the transition strain as a function of Z .

fraction of DRX is also corresponding to the decoration of all the pre-existing grain boundaries by the new DRX grains. Therefore, it can be concluded that a minimum fraction of DRX microstructure is necessary for a transition from strain dependent to strain independent occurs during un-loading of the deformed material.

The microstructures produced by quenching after different un-loading times (Fig. 12) showed that some new small recrystallized grains formed during the annealing. These recrystallized grains formed predominantly on the serrated pre-existing grain boundaries. The effect of strain and un-loading time on the post-DRX microstructure can be traced by their effect on the grain size (Fig. 14). The average grain size (including both recrystallized and deformed grains) decreased with increasing un-loading time to a minimum value, where the time to this value depended on the strain, and then increased with increasing time. The relative depth of this minimum point (i.e. d_{min}/d_0) decreased with increasing strain (or increasing DRX fraction) and was generally when 20% softening had occurred. However at very high strains, the minimum in the curve for the high strain ($\varepsilon = 2$), where more than 80% of microstructure had recrystallized during deformation (Fig. 6e), is negligible and in this case the major change in the microstructure occurred after 50% softening.

The decrease and then increase in the average grain size with increasing un-loading time can be attributed to the formation of

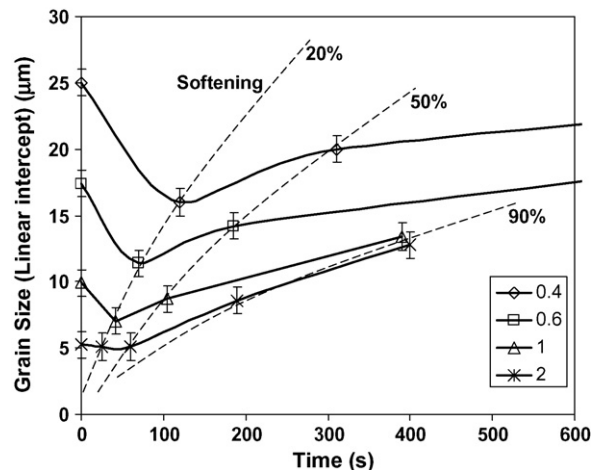


Fig. 14. The average grain size (linear intercepts) as a function of un-loading time at different strains, for deformation at 900°C and a strain rate of 0.01 s^{-1} .

new small SRX and post-DRX grains and the growth of these grains, respectively. At the short times and lower strains, many new small grains are formed and the average grain size decreases. After a certain time, which is a function of strain, most of the deformed microstructure is replaced by newly formed grains and grain growth occurs with longer annealing time (Fig. 12f and i), and the average grain size increases with increasing the time. However, at large strains it would appear that the process mostly involves growth of the microstructure. Fig. 14 indicates that grain growth has an important role in the post-DRX and, in fact, this mechanism (i.e. grain growth) can be responsible for most fraction of softening during un-loading (especially at higher strains). This has been noted in earlier work related to the metadynamic recrystallization of C–Mn steel [45].

5. Conclusions

The hot deformation and recrystallization of a 304 austenitic stainless steel was examined in torsion where it was found that:

- i. Both peak and critical strains are power law functions of Zener–Hollomon, Z , parameter and ratio of critical to the peak strain is 0.6.
- ii. The dependency of time for 50% recrystallization (t_{50}) changes from strain dependent to strain independent at a transition strain (ε^*) far beyond the peak. The dependency of this transition strain to temperature is more obvious than its dependency to strain rate.
- iii. The transition strain, ε^* , clearly links to the strain for almost 50% DRX during deformation. On the other hand, that 50% recrystallization obtains by completion of the first layer of necklace structure (i.e. decoration of all initial grain boundaries by DRX grains).
- iv. The softening kinetics of deformed material in the strain independent area (i.e. at $\varepsilon \geq 1.5$) is very similar to the recrystallization kinetics during deformation, indicating similarity between DRX and post-DRX kinetics.
- v. The present results clarify the important role of grain growth on post-deformation softening of a deformed microstructure. This role increases by increasing strain of the hot deformed material.

References

- [1] F.J. Humphreys, M. Hatherly, *Recrystallization and Related Annealing Phenomena*, first ed., Pergamon, Oxford, 1996.
- [2] D. Ponge, G. Gottstein, *Acta Mater.* 46 (1998) 69–80.
- [3] C.M. Sellars, in: C.M. Sellars, C.H.J. Davies (Eds.), *Proceedings of Hot Working and Forming Process*, The Metal Society, London, England, 1979, pp. 3–15.
- [4] T. Maki, S. Okaguchi, I. Tamura, in: H.J. McQueen (Ed.), *Proceedings of the 7th International Conference on the Strength of Metals and Alloys (ICSMA 7)*, Montreal, Canada, 1985, pp. 923–928.
- [5] M. Ueki, S. Horie, T. Nakamura, *Mater. Sci. Technol.* 3 (1987) 329–337.
- [6] T. Sakai, J.J. Jonas, *Acta Metall.* 32 (1984) 189–209.
- [7] A. Belyakov, H. Miura, T. Sakai, *Scripta Mater.* 43 (2000) 21–26.
- [8] G. Gottstein, E. Brunger, D. Ponge, in: J.J. Jonas, T.R. Bieler, K.J. Bowman (Eds.), *Proceedings of Advanced in Hot Deformation Textures and Microstructures*, TMS, USA, 1993, pp. 477–492.
- [9] P.D. Hodgson, in: T. Chandra, T. Sakai (Eds.), *Proceedings of International Conference on Thermomechanical Processing of Steels & Other Materials, Thermec'97*, The Minerals, Metals & Materials Society, Wollongong, Australia, 1997, pp. 121–131.
- [10] P.D. Hodgson, R.E. Gloss, G.L. Dunlop, in: M.E. Kassner (Ed.), *Proceedings of 32nd Mechanical Working and Steel Processing, Iss-AIME*, Warrendale, Pennsylvania, 1990, pp. 527–538.
- [11] C. Roucoules, P.D. Hodgson, *Mater. Sci. Technol.* 11 (1995) 548–556.
- [12] A.R. Morgridge, *Bull. Mater. Sci.* 25 (2002) 291–299.
- [13] P.D. Hodgson, *Mathematical Modelling of Recrystallization Processes During the Hot Rolling of Steel*, Department of Mining and Metallurgical Engineering, University of Queensland, 1993.
- [14] C. Roucoules, P.D. Hodgson, S. Yue, J.J. Jonas, *Metall. Mater. Trans. A* 25 (1994) 389–400.
- [15] W.P. Sun, E.B. Hawbolt, *ISIJ Int.* 37 (1997) 1000–1009.
- [16] A.M. Elwazri, P. Wanjara, S. Yue, *ISIJ Int.* 43 (2003) 1080–1088.
- [17] C. Devidas, I.V. Samarasekera, E.B. Hawbolt, *Metall. Trans. A* 22A (1991) 335–349.
- [18] L.P. Karjalainen, T.M. Maccagno, J.J. Jonas, *ISIJ Int.* 35 (1995) 1523–1531.
- [19] J.J. Jonas, *ISIJ Int.* 40 (2000) 731–738.
- [20] B. Derby, M.F. Ashby, *Scripta Metall.* 21 (1987) 879–884.
- [21] J.J. Jonas, T.M. Maccagno, S. Yue, in: E.B. Hawbolt, S. Yue (Eds.), *Proceedings of International Symposium on Phase Transformations During the Thermal/Mechanical Processing of Steel*, The Metallurgical Society of CIM, Vancouver, Canada, 1995, pp. 179–193.
- [22] T. Sakai, *J. Mater. Proc. Technol.* 53 (1995) 349–361.
- [23] A. Dehghan-Manshadi, H. Beladi, M.R. Barnett, P.D. Hodgson, *Mater. Forum* 467–470 (2004) 1163–1168.
- [24] A. Dehghan-Manshadi, *The Evolution of Recrystallization During and Following Hot Deformation*, PhD Thesis, School of Engineering and IT, Deakin University, Geelong, Victoria, 2007.
- [25] S. Venugopal, S.L. Mannan, *Mater. Sci. Eng. A* 177 (1994) 143–149.
- [26] I. Salvatori, T. Inoue, K. Nagai, *ISIJ Int.* 42 (2002) 744–750.
- [27] N.D. Ryan, H.J. McQueen, *Can. Metall. Quart.* 29 (1990) 147–162.
- [28] H. Weiss, D.H. Skinner, J.R. Everett, *J. Phys. E* 6 (1973) 709–712.
- [29] A. Laasraoui, J.J. Jonas, *Metall. Trans. A* 22A (1991) 151–160.
- [30] M.L. Bernshtein, L.M. Kapltkina, S.D. Prokoshkin, S.V. Dobatkin, *Acta Metall.* 33 (1985) 247–254.
- [31] E.I. Poliak, J.J. Jonas, *Acta Mater.* 44 (1996) 127–136.
- [32] C.M. Sellars, W.J. McGart, *Acta Metall.* 14 (1966) 1136–1138.
- [33] A. Belyakov, H. Miura, T. Sakai, *Mater. Sci. Eng. A* 255 (1998) 139–147.
- [34] S.I. Kim, Y.C. Yoo, *Mater. Sci. Eng. A* 311 (2001) 108–113.
- [35] X. Wang, E. Brunger, G. Gottstein, *Scripta Mater.* 46 (2002) 875–880.
- [36] H. Miura, T. Sakai, H. Hamji, J.J. Jonas, *Scripta Mater.* 50 (2004) 65–69.
- [37] T. Sakai, A. Belyakov, H. Miura, in: G. Gottstein, D.A. Molodov (Eds.), *Proceedings of the First Joint International Conference on Recrystallization and Grain Growth*, Springer-Verlag, Aachen, Germany, 2001, pp. 669–682.
- [38] W. Roberts, B. Ahlborn, *Acta Metall.* 26 (1978) 801–813.
- [39] E. Brunger, X. Wang, G. Gottstein, *Scripta Mater.* 38 (1998) 1843–1849.
- [40] J.P. Sah, C.J. Richardson, C.M. Sellars, *Met. Sci.* 8 (1974) 325–331.
- [41] W. Roberts, H. Benden, B. Ahlborn, *Met. Sci.* 13 (1979) 195–203.
- [42] A. Belyakov, T. Sakai, H. Miura, R. Kaibyshev, *ISIJ Int.* 39 (1999) 592–599.
- [43] P. Uranga, A.I. Fernandez, B. Lopez, J.M. Rodriguez-Ibabe, *Mater. Sci. Eng. A* 345 (2003) 219–327.
- [44] M.R. Cartmill, M.R. Barnett, S.H. Zahiri, P.D. Hodgson, *ISIJ Int.* 45 (2005) 1903–1908.
- [45] C. Roucoules, *Dynamic and Metadynamic Recrystallization in HSLA Steels*, Department of Mining and Metallurgical Engineering, McGill University, Montreal, Canada, 1992.
- [46] J.H. Beynon, C.M. Sellars, *ISIJ Int.* 32 (1992) 359–367.
- [47] C.M. Sellars, in: N. Hansen, D. Jull Jensen, T. Leffers, B. Ralph (Eds.), *Proceedings of Annealing Processes—Recovery, Recrystallization and Grain Growth (7th Riso International Symposium on Metallurgy and Materials Science)*, Riso National Laboratory, Roskilde, Denmark, 1986, pp. 167–187.